Available online at www.sciencedirect.com
ScienceDirect
Physica A 374 (2007) 127–138
PHYSICA A
www.elsevier.com/locate/physa

The transverse spin-$\frac{1}{2}$ Ising order-disorder superlattice

M. Saber[a,b,c,*], I. Lukyanchuk[c], M. Madani[a], A. Tabyaoui[a], A. Ainane[a,b,c]

[a]*Max Planck Institut für Physik Komplexer Systeme Nöthnitzer Str. 38, D-01187, Dresden, Germany*
[b]*Physics Department, Faculty of Sciences, University of Moulay Ismail, B.P. 11201, Meknes, Morocco*
[c]*Laboratoire de Physique de la Matière Condensée Département de Physique, Faculté des Sciences, Université Picardie, F-80039 Amiens Cedex, France*

Received 11 June 2005; received in revised form 26 March 2006
Available online 10 November 2006

Abstract

We apply the Ising model in a transverse field to analyse the properties of $KH_2PO_4/KD_2H_2PO_4$ superlattice using the effective field theory with a probability distribution technique. The dielectric-susceptibility and the macroscopic pyroelectric coefficient are calculated for possible comparison with experimental data. We show for thick layer superlattices, two peaks in the mean dielectric susceptibility and pyroelectric coefficient, as they had two phase transitions, whereas thin-layer superlattices, show one-peak behavior.

Keywords: Ferroelectric; Dielectric response; Phase transitions

1. Introduction

The dependence of ferroelectric behavior on the size and the film thickness effects has been investigated theoretically [1–3] and experimentally [4,5] for a long time. In recent years, the interest in size effects on ferroelectricity was inspired by problems in microelectronics for instance by using materials in nonvolatile memory devices. In addition, recent development of ferroelectric films or superlattices has made them to a subject of practical relevance.

From the theoretical point of view, the Landau–Devonshire theory of ferroelectric phase transitions has been extended for the description of thin films [6–8], and ferroelectric superlattices [9–13], which are of increasing importance. One problem with this approach is that it is not clear how to account for the coupling between layers within a continuum theory. Approaches based on the Ising model in a transverse field [14,15] have the advantage that this coupling is automatically described by an inter-layer exchange coupling. In the last decades, there has been an interesting number of works dealing with the critical behavior of quantum spin systems. The transverse Ising model is the simplest quantum system and has been introduced to explain the phase transition of hydrogen-bonded ferroelectrics such as KH_2PO_4 and other systems (a more detailed application has been reviewed in Ref. [16]) for instance the order-disorder phenomenon with tunnelling effects.

*Corresponding author. Physics Department, Faculty of Sciences, University of Moulay Ismail, B.P. 11201, Meknes, Morocco.
E-mail address: saber@mpipks-dresden.mpg.de (M. Saber).

0378-4371/$ - see front matter © 2006 Elsevier B.V. All rights reserved.
doi:10.1016/j.physa.2006.05.058

Since then, it has been successfully applied to several physical systems, such as a cooperative Jahn–Teller system [17] (like $DyVO_4$ and $TbVO_4$), ordering in rare earth (RE) compounds with a crystal-field ground state [18], and also to some real magnetic materials with strong uniaxial anisotropy in a transverse field [19].

Ferroelectrics with the basic KH_2PO_4 crystal structure have attracted an enormous amount of interest over several decades and recently they have been used as common examples of order-disorder ferroelectrics [20]. From an experimental standpoint the reasons are practical, large single crystals can be grown easily from water solution and they are in general of high optical quality. As a result they yield useful technological devices such as high-speed electro-optic modulators. Theoretically, the occurrence of ferroelectricity in these materials is associated in a large degree with proton tunelling, but a strong coupling to the hear [21]. A KH_2PO_4/KD_2PO_4 (KDP/KD^*P) superlattice is a particularly simple example because the transverse field is nearly the same in both constituents and only the exchange interaction changes significantly at the interface. Our aim in this paper is to study the dielectric and pyroelectric properties of a $(KDP)_{L_A}/(KD^*P)_{L_B}$ using the transverse spin-$\frac{1}{2}$ Ising superlattice within the framework of the effective field theory with a probability distribution technique [22] that accounts for the self-spin correlations functions. This technique is believed to give more quantitatively exact results than the standard mean field approximation and it has the same qualitatively behavior as it [22]. In Section 2, we give the equations that determine the polarizations and the critical temperature of the superlattice as functions of exchange interactions, transverse field and superlattice thickness. The dielectric susceptibility and the pyroelectric coefficient are discussed in Section 3, and a brief conclusion is given in Section 4. Our results are in good agreement with those obtained recently by Wang et al. [23].

2. Model and formalism

We consider a superlattice consisting of two different ferromagnetic materials KDP and KD^*P stacked alternately. For simplicity, we restrict our attention to the case of the simple cubic structure. The periodic condition suggests that we only have to consider one unit cell. A model of $(KDP)_3/(KD^*P)_3$ is depicted in Fig. 1. The exchange coupling between the nearest-neighbor spins in KDP (KD^*P) is denoted by J_A (J_B), while the transverse field is expressed by Ω_i. Here, we consider the interface to be composed of two layers (L_A and L_A+1). J_{AB} stands for the exchange coupling between the nearest-neighbor spins across the interface. The number of atomic layers in the KDP (KD^*P) material is L_A (L_B) and the thickness of the cell is $L=L_A+L_B$. The Hamiltonian of this system is given by

$$H=-\sum_{(i,j)} J_{ij}\sigma_i^z\sigma_j^z-\sum_i \Omega_i\sigma_i^x, \tag{1}$$

where σ_{iz} and σ_{ix} denote the z and x components of a quantum spin $\vec{\sigma}_i$ of magnitude $\sigma=\frac{1}{2}$ at site i. The first sum runs over all nearest-neighbor pairs, the second sum is taken over the spins and J_{ij} stands for one of the three coupling (J_A, J_B, J_{AB}) depending on the location of the spin pairs. Using the effective field theory [22], the nth layer longitudinal and transverse polarizations of the superlattice are derived in the same manner as for the transverse spin-$\frac{1}{2}$ Ising superlattice [24] and they are given by

$$\begin{aligned} p_{n\alpha}=2^{-N-2N_0}\sum_{\mu=0}^{N}\sum_{\mu_1=0}^{N_0}\sum_{\mu_2=0}^{N_0}\Big\{ & C_\mu^N C_{\mu_1}^{N_0} C_{\mu_2}^{N_0}(1-2p_{nz})^{\mu}(1+2p_{nz})^{N-\mu} \\ & \times(1-2p_{n-1,z})^{\mu_1}(1+2p_{n-1,z})^{N_0-\mu_1}(1-2p_{n+1,z})^{\mu_2}(1+2p_{n+1,z})^{N_0-\mu_2} \\ & \times f_\alpha\left(\frac{1}{2}[J_{n,n}(N-2\mu)+J_{n,n-1}(N_0-2\mu_1)+J_{n,n+1}(N_0-2\mu_2)],\Omega_n\right)\Big\}, \end{aligned} \tag{2}$$

where

$$f_z(y,\Omega_n)=\frac{1}{2}\frac{y}{(y^2+\Omega_n^2)^{1/2}}\tanh\left[\frac{1}{2}\beta(y^2+\Omega_n^2)^{1/2}\right] \tag{3}$$

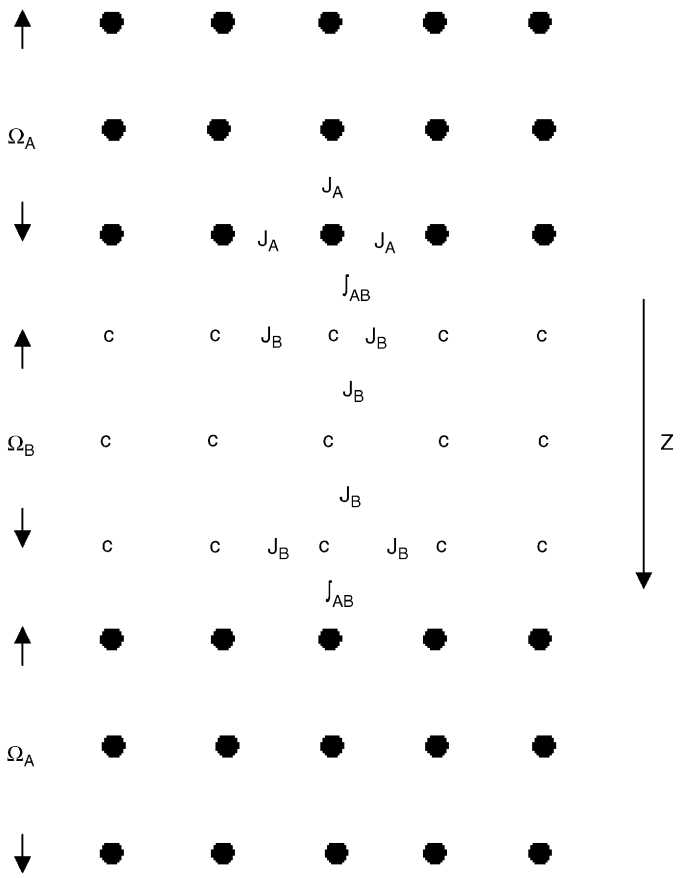

Fig. 1. Schematic diagram of three layers of the KDP/KD^*P superlattice. The exchange constant are J_A in the KDP layers, J_B in the KD^*P layers and $J_{AB} = (J_A + J_B)/2$ across the interfaces. The transverse fields are Ω_A and Ω_B.

and

$$f_x(y, \Omega_n) = f_z(\Omega_n, y) \tag{4}$$

with

$$y = \tfrac{1}{2}[J_{n,n}(N - 2\mu) + J_{n,n-1}(N_0 - 2\mu_1) + J_{n,n+1}(N_0 - 2\mu_2)], \tag{5}$$

where $\alpha = z(x)$ for the longitudinal (transverse) polarization and $n = 1, 2, \ldots, L_A - 1, L_A, L_A + 1, \ldots, L_A + L_B - 1, L = L_A + L_B$. N and N_0 are the numbers of the nearest neighbors in the plane and between adjacent planes, respectively. C_k^l are the binomial coefficients, $C_k^l = \frac{l!}{k!(l-k)!}$. The periodic condition of the superlattice has to be satisfied, namely, $p_{0\alpha} = p_{L\alpha}$ and $p_{L+1,\alpha} = p_{1,\alpha}$.

For the case of a simple cubic lattice which we will consider here, one has $N = 4$ and $N_0 = 1$. The same equations hold for an arbitrary superlattice structure with a coordination number, $N + 2N_0$, and therefore results for different structures can be obtained without carrying out the detailed algebra encountered when employing other techniques. The longitudinal and transverse polarizations of the superlattice are defined by

$$p_\alpha = \frac{1}{L}\sum_{n=1}^{L} p_{n\alpha}. \tag{6}$$

We have thus obtained the self-consistent equations (2) for the layer longitudinal and transverse polarizations p_{nz} and p_{nx} that can be solved directly by numerical iteration. As we are interested with the calculation of the longitudinal ordering near the transition critical temperature, the usual argument that the layer longitudinal

polarization p_{nz} tends to zero as the temperature approaches its critical value T_c, allows us to consider only terms linear in p_{nz} because higher order terms tend to zero faster than p_{nz} on approaching a critical temperature T_c. Above T_c the ferroelectric phase does not exist. The language often used is this: below T_c the ferroelectric is in a ferroelectric phase, above T_c it is in the paraelectric phase. Consequently, all terms of the order higher than linear terms in Eq. (2) can be neglected. This leads to the set of simultaneous equations

$$p_{nz} = A_{n,n-1}p_{n-1,z} + A_{n,n}p_{nz} + A_{n,n+1}p_{n+1,z} \tag{7}$$

which can be written as

$$M\vec{p_z} = 0, \tag{8}$$

where $\vec{p_z}$ is a vector of components $(p_{1z},\ldots,p_{nz},\ldots,p_{Lz})$ and M is a matrix of elements

$$M_{i,j} = (A_{i,i} - 1)\delta_{i,j} + A_{i,j}(\delta_{i,\,j-1} + \delta_{i,\,j+1}). \tag{9}$$

The only nonzero elements of the matrix M are given by

$$M_{n,n-1} = 2^{-N-2N_0}\sum_{\mu=0}^{N}\sum_{\mu_1=0}^{N_0}\sum_{\mu_2=0}^{N_0}\sum_{i=0}^{\mu_1}\sum_{j=0}^{N_0-\mu_1}[(-1)^i 2^{i+j}\delta_{1,i+j}\times C_\mu^N C_{\mu_1}^{N_0} C_{\mu_2}^{N_0} C_i^{\mu_1} C_j^{N_0-\mu_1} f_z(y_n,\Omega)], \tag{10}$$

$$M_{n,n} = 2^{-N-2N_0}\sum_{\mu=0}^{N}\sum_{\mu_1=0}^{N_0}\sum_{\mu_2=0}^{N_0}\sum_{i=0}^{\mu}\sum_{j=0}^{N_0-\mu}[(-1)^i 2^{i+j}\delta_{1,i+j}\times C_\mu^N C_{\mu_1}^{N_0} C_{\mu_2}^{N_0} C_i^{\mu} C_j^{N-\mu} f_z(y_n,\Omega)] - 1, \tag{11}$$

$$M_{n,n+1} = 2^{-N-2N_0}\sum_{\mu=0}^{N}\sum_{\mu_1=0}^{N_0}\sum_{\mu_2=0}^{N_0}\sum_{i=0}^{\mu_2}\sum_{j=0}^{N_0-\mu_2}[(-1)^i 2^{i+j}\delta_{1,i+j}\times C_\mu^N C_{\mu_1}^{N_0} C_{\mu_2}^{N_0} C_i^{\mu_2} C_j^{N_0-\mu_2} f_z(y_n,\Omega)] \tag{12}$$

with the periodic boundary conditions $M_{1,0} = M_{1,L}$ and $M_{L,L+1} = M_{L,1}$. All the information about the critical temperature of the system is contained in Eq. (7). Up to now we did not assign precise values of the exchange interactions and the strength of the transverse field and unit cell width: the terms in matrix (7) are general ones.

In a general case, for arbitrary exchange interactions, transverse field and unit cell width, the evaluation of the critical temperature relies on numerical solution of the system of linear equations (7). These equations can be satisfied by nonzero polarization vectors $\vec{p_z}$ only if

$$\det M = 0. \tag{13}$$

In general, Eq. (13) can be satisfied for $L = L_A + L_B$ different values of the critical temperature T_c from which we choose the one corresponding to the highest possible transition temperature (see discussion in Ref. [25]). This value of T_c corresponds to a solution having $p_{1z}, p_{2z},\ldots,p_{Lz}$ positive, which is compatible with a longitudinal ordering. The other formal solutions correspond in principle to other types of ordering that usually do not occur here [25].

The dielectric properties are important in practice and in particular the longitudinal dielectric susceptibilities are interesting physical quantities which describe the characteristics of the change of the polarizations with the fields and can show the phase transition properties, particularly its critical temperature T_c. The longitudinal dielectric susceptibility χ_z is a quantity related to how easily the longitudinal polarization responds to an external electric field E. The phase transition is usually predicted by the abnormal behavior of the longitudinal dielectric susceptibility at the critical temperature. In order to obtain the longitudinal dielectric susceptibility, we apply a uniform longitudinal electric field E across the superlattice, which adds to the Hamiltonian equation (1) a term

$$H_1 = -E\sum_{i=1}^{L}\sigma_{iz} \tag{14}$$

describing the interaction of the longitudinal polarization with the electric field E. In order to calculate the longitudinal dielectric susceptibility, we apply the formalism of Section 2. Eq. (2) continue to apply but the parameter y now is replaced by $y + E$. The longitudinal dielectric susceptibility of the nth layer is

given by

$$\chi_{nz} = \frac{\partial p_{nz}}{\partial E}\bigg)_{h=0}. \tag{15}$$

The details of the calculus of the layer longitudinal dielectric susceptibilities are given in the Appendix. To evaluate the longitudinal dielectric susceptibility of the superlattice, we follow the formalism of Wang et al. [26]. As each layer can be treated as a capacitor, the capacitance of the superlattice is the sum of the capacitances of each of the layers connected in series. The total reciprocal permittivity is the sum of the reciprocal permittivities at each of the layers. Thus, the total longitudinal dielectric susceptibility (the longitudinal dielectric susceptibility of the superlattice) χ_z is determined from

$$(1+\chi_z)^{-1} = \frac{1}{L}\sum_{n=1}^{L}(1+\chi_{nz})^{-1}, \tag{16}$$

where L is the total number of layers.

The pyroelectric coefficient of the nth layer is defined by

$$P_{nz} = \frac{\partial p_{nz}}{\partial T}. \tag{17}$$

The mean pyroelectric coefficient of the superlattice is given by

$$P_z = \frac{\partial p_z}{\partial T} = \frac{1}{L}\sum_{n=1}^{L}\frac{\partial p_{nz}}{\partial T}, \tag{18}$$

where L is the total number of layers ($L = L_A + L_B$).

The derivation $\partial p_{nz}/\partial T$ can be obtained by numerical differential calculation, then P_{nz} and P_z are obtained numerically.

3. Results and discussion

In this section we perform numerical analysis of the obtained theoretical results for the thermodynamic and static characteristics of the order-disorder KDP/KD^*P superlattice. Our goal is the study of the temperature dependence of the above theoretical physical quantities.

In bulk material all Ω_i are equal and in the nearest-neighbor exchange approximation with all exchange constants equal to J, the bulk longitudinal polarization of the system is given by

$$p_z = 2^{-N-2N_0}\sum_{\mu=0}^{N}\sum_{\mu_1=0}^{N_0}\sum_{\mu_2=0}^{N_0} C_\mu^N C_{\mu_1}^{N_0} C_{\mu_2}^{N_0}(1-2p_z)^{\mu+\mu_1+\mu_2}(1+2p_z)^{N+2N_0-\mu-\mu_1-\mu_2} f_z(y,\Omega). \tag{19}$$

The bulk critical temperature T_c is determined as the highest temperature at which Eq. (19) for the bulk longitudinal polarization p_z has a nontrivial solution. In other words, when Eq. (19) is expanded into power series of p_z, the coefficient of the linear term of p_z in the right-hand side is equal to unity at $T = T_c$. Thus the equation for T_c becomes

$$1 = 2^{-N-2N_0}\sum_{\mu=0}^{N}\sum_{\mu_1=0}^{N_0}\sum_{\mu_2=0}^{N_0}\sum_{i=0}^{\alpha_1}\sum_{j=0}^{\alpha_2} C_\mu^N C_{\mu_1}^{N_0} C_{\mu_2}^{N_0} C_i^{\alpha_1} C_j^{\alpha_2}(-1)^i 2^{i+j}\delta_{i+j,1} f_z(y,\Omega) \tag{20}$$

with $\alpha_1 = \mu+\mu_1+\mu_2$, $\alpha_2 = N+2N_0-(\mu+\mu_1+\mu_2)$ and $y = \frac{1}{2}J(\alpha_2-\alpha_1)$.

Eq. (20) yields

$$\tfrac{3}{8}f_z(3J,\Omega) + \tfrac{3}{2}f_z(2J,\Omega) + \tfrac{15}{8}f_z(J,\Omega) = 1. \tag{21}$$

On the other hand, the transverse field Ω is a measure of the tunnelling probability of the proton or deuteron between the two potential minima in a hydrogen. To be precise, the critical temperature for KDP is $T_c^A = 123\,\mathrm{K}$ and for KD^*P is $T_c^B = 213\,\mathrm{K}$. As seen from Eq. (21), the values of J and Ω for a given material are related by the value of T_c. With the use of book value [11], $\Omega_A = 383\,\mathrm{K}$ for KDP we find $J_A = 173\,\mathrm{K}$.

To determine the parameters for KD^*P we make use of the effective field expression for the zero-temperature longitudinal bulk polarization $p_z(T=0)$, namely

$$p_z(T=0) = \frac{1}{2\left[1+(\Omega/3J)^2\right]^{1/2}} \tag{22}$$

together with the value $p_z^A(T=0)/p_z^B(T=0) = 1.24$ which is equal to the corresponding ratio of polarizations. This numerical ratio, combined with Eq. (21) for T_c and the parameters values for KDP enable us to determine that for KD^*P we obtain $J_B = 197\,\mathrm{K}$ and $\Omega_B = 292\,\mathrm{K}$. We consider a $(KDP)_{L_A}/(KD^*P)_{L_B}$ superlattice of the form shown in Fig. 1, corresponding to growth in the z-direction. The interface exchange constant J_{AB} is not known and we simply put $J_{AB} = (J_A + J_B)/2$. Our results are unlikely to be much affected by the precise value chosen for J_{AB}.

The critical temperature of the superlattice T_{cs} versus layer numbers L_A and L_B is shown in Fig. 2. The bulk critical temperature T_c is lower for KDP than for KD^*P as is to be expected. It is found that for fixed values of the thickness L_A, the critical temperature T_{cs} of the superlattice increases with increasing the thickness L_B, and for fixed L_B, T_{cs} increases with increasing L_A. The critical temperature of the superlattice depends sensitively upon the period of the superlattice when it is small. The smaller the period, the lower the critical temperature T_{cs}. The critical temperature of the superlattice approaches the bulk critical temperature of material B when the period becomes very large.

The layer site dielectric susceptibility is shown in Fig. 3. We calculated its values for the 25/25 (Fig. 3a) and 5/5 (Fig. 3b) superlattices. The striking feature of Fig. 3a is that in the KDP layer the mid-layer value of site dielectric susceptibility becomes large at $T = 0.5T_c^B$, whereas in the KD^*P layer site the dielectric susceptibility increases monotonically with the temperature. In Fig. 3b, on the other hand, the mid-KDP value of site the dielectric susceptibility is enhanced at $T = 0.5T_c^B$ compared with $T = 0.1T_c^B$, but the value for $T = 0.9T_c^B$ is somewhat larger. These characteristics arise because in the bulk material the susceptibility diverges at the critical temperature, which is near $T = 0.5T_c^B$ for KDP and at $T = T_c^B$ for KD^*P. Within the thicker KDP layer, Fig. 3a, but not in the thinner KDP layer of Fig. 3b, the site dielectric susceptibility rises to near the bulk value at $T = 0.5T_c^B$. The divergence of susceptibility in KD^*P at $T = T_c^B$ accounts for the relatively large values of site dielectric susceptibility within the KD^*P layer at $T = 0.9T_c^B$ and is also seen to pull up the values in the KDP layer.

For the sake of illustration, we have calculated the mean susceptibility, and its temperature dependence is shown in Fig. 4. In the 25/25 superlattice two peaks are seen, one just above the bulk critical temperature of

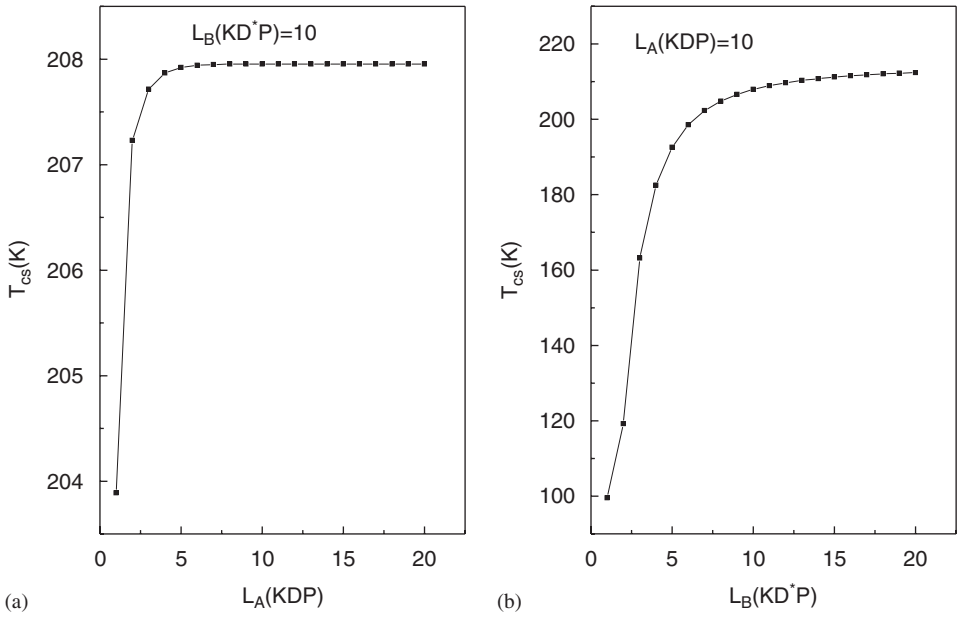

Fig. 2. Critical temperature T_{cs} of the $(KDP)_{L_A}/(KD^*P)_{L_B}$ superlattice versus (a) L_A when $L_B = 10$ and (b) L_B when $L_A = 10$.

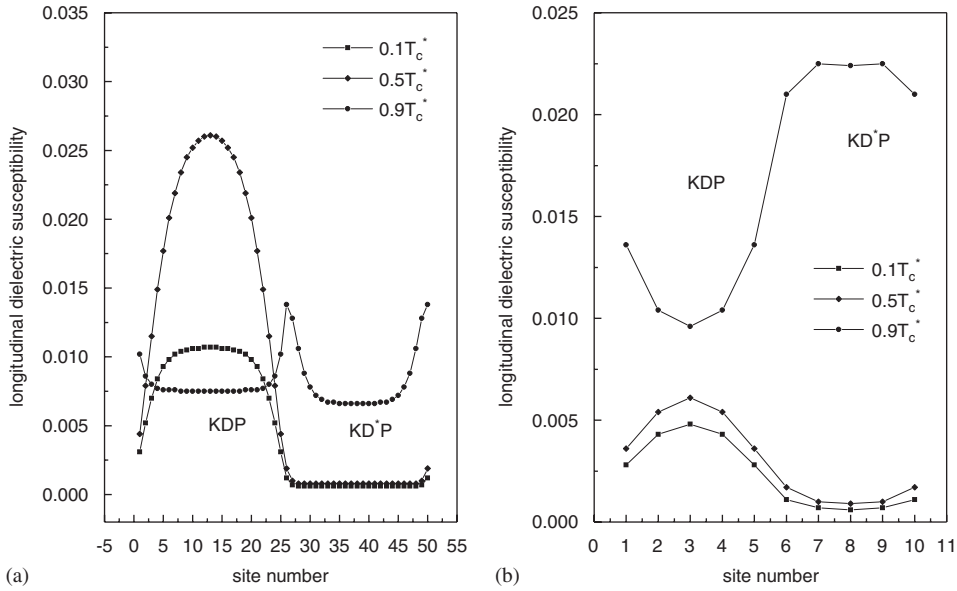

Fig. 3. The profiles of the longitudinal susceptibility for a (a) $(KDP)_{25}/(KD^*P)_{25}$ and (b) $(KDP)_5/(KD^*P)_5$ superlattice at different temperatures, $T = 0.1T_c^B$, $T = 0.5T_c^B$, $T = 0.9T_c^B$. Temperatures are given in terms of the bulk KD^*P Curie temperature $T_c^B = 213\,\mathrm{K}$.

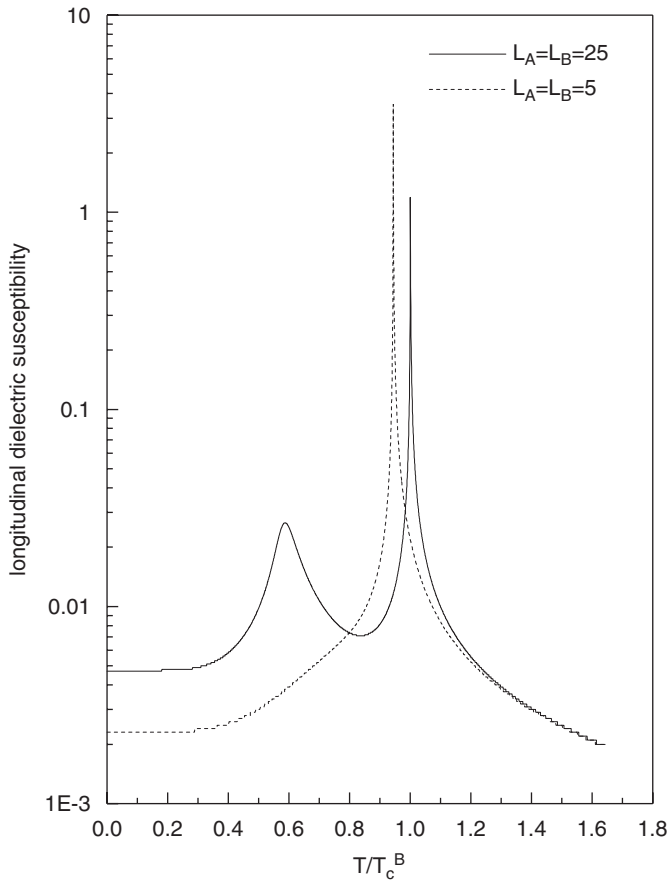

Fig. 4. The temperature dependence of the mean susceptibility. Dashed for $(KDP)_5/(KD^*P)_5$ superlattices and solid for $(KDP)_{25}/(KD^*P)_{25}$ superlattices.

KDP and a stronger and sharper one at the superlattice critical temperature T_{cs}. The former derives from the increase in the mid-layer site dielectric susceptibility seen in Fig. 3a and the latter is the expected divergence at T_{cs}. In the 5/5 superlattice, only the critical divergence is seen with a weak anomaly near T_c^A. These characteristics are easily related to Fig. 3b.

With a view to possible experiments we have also calculated, by numerical differentiation, the pyroelectric coefficient and the results for our two example superlattices are shown in Fig. 5. The pyroelectric coefficient of the superlattice shows a sharp peak at the critical temperature of the superlattice which has been found theoreticaly in Ref. [27] using the mean field approach for the transverse Ising model and also it has been observed in the experimental results [28]. Two pyroelectric peaks are found for large period superlattices (25/25). The pyroelectric peak at low temperature disappears when the period is very small (5/5). The general forms of these curves are similar to those in Fig. 4 and they can be interpreted in a similar way.

There has been a small number of previous theoretical papers in which the transverse Ising model was applied to ferroelectric superlattices. In particular, Wang and Smith [14] consider a superlattice in which the transverse field Ω is the same in both components but the exchange coupling J takes different values. Wang et al. [15] discuss a general multilayer system for the Curie temperature that can be solved in this general case by a transfer-matrix method. Wang et al. [29] apply the same approach as we use here for a three layers superlattice. Qu et al. [11] start from the Ising Hamiltonian with a transverse field in rather general form, including fourth-order terms, and use a continuum approximation to establish exactly the form of the Landau–Devonshire expansion.

Experimental results on a $BaTiO_3/SrTiO_3$ superlattice were reported by Qu et al. [30]. Their results on samples with total thickness of 400 nm show behavior similar to that of relaxor ferroelectrics and it seems

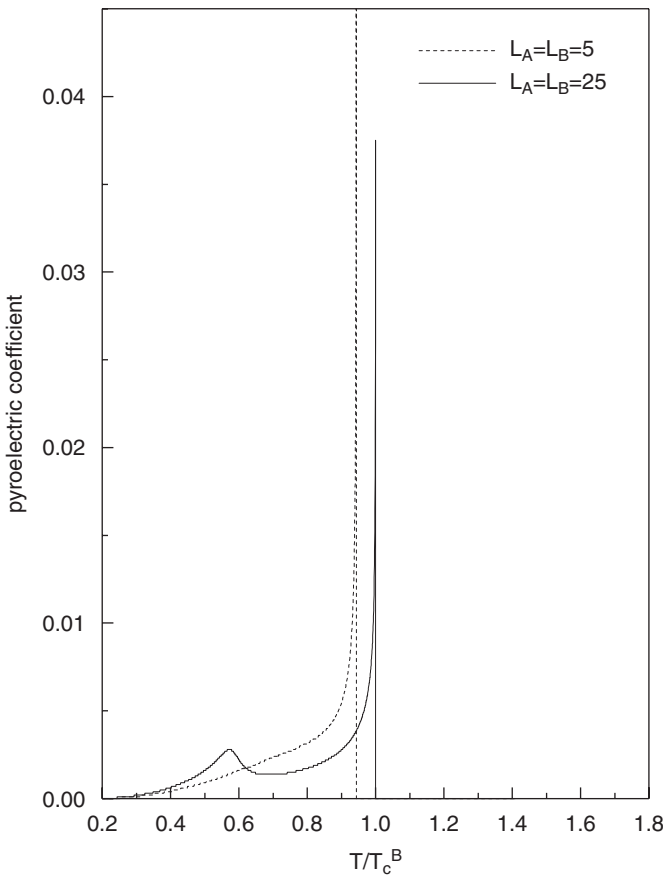

Fig. 5. The temperature dependence of the pyroelectric coefficient. Dashed for $(KDP)_5/(KD^*P)_5$ superlattices and solid for $(KDP)_{25}/(KD^*P)_{25}$ superlattices.

unlikely that these results can be explained by the kind of model we have presented here. However, for total thickness of 800 nm, the measured dielectric constant has either a two-peak or a one-peak form depending on the size of the superlattice unit cell. $BaTiO_3$ and $SrTiO_3$ are displacive ferroelectrics and therefore better described by the Landau–Devonshire theory. Calculations within this framework [11] agree qualitatively with the experimental measurements. There are similar results in the magnetism literature. Ramos et al. [31] used high-quality epitaxial deposition to prepare superlattices of the fluoride antiferromagnets FeF_2/CoF_2. By means of high-resolution X-ray diffraction they measured the thermal expansion coefficient α. Because of magneto-elastic coupling to the magnetic susceptibility, this shows peaks at magnetic transition temperatures. They found that for thick-layer superlattices, and by implication the susceptibility, shows two peaks, one near to $T_c(FeF_2)$ and one near to $T_c(CoF_2)$. In thin-layer superlattices, on the other hand, only one peak was observed at a temperature intermediate between $T_c(FeF_2)$ and $T_c(CoF_2)$. Numerical simulations to compare with these results were performed by Carrico and Camely [32] using numerical mean-field theory on a Heisenberg Hamiltonian, and by Wang and Mills [33] within a Landau-theory formulation. In a similar way to our Figs. 4 and 5, these simulations confirm the one-peak form for thin layers and the two-peak form for thicker layers. To be pedantic, one should say that in any superlattice, however, thick the layers, there is only one critical temperature, which coincides with the position of the higher peak in graphs like Fig. 4 or 5. However, there is no great harm in the statement that two phase transitions are seen for thick layers and only one for thin layers since this describes the peaks in the temperature dependence of mean susceptibility and pyroelectric coefficient.

4. Conclusion

By making use of the effective field theory with a probability distribution technique, we have studied a ferroelectric superlattice consisting of two coupled ferroelectric sublattices. It is described by the transverse Ising model, which takes into account the effect of the number of layers and the critical temperature. We can show that for thick layer superlattices, two peaks in mean susceptibility and pyroelectric coefficient, but for thin layer superlattices, one peak is obtained. When its period is large or small, it is still having ferroelectric features. The results obtained are qualitatively similar to those obtained in Ref. [23].

Acknowledgments

Two of the authors A.A. and M.S. gratefully acknowledge the hospitality of the Max Planck Institut für Physik Komplexer Systeme Dresden, Germany where this work has been initiated and the Picardie University, Amiens, France where it has been completed with the support of PROTATRS III D1208 and the Nato Support (Collaborative Linkage Grant project on "New Ferroelectric-Relaxor Oxydes for Microelectronic Applications") Reference: PST.CLG 980055.

Appendix A. Calculation of the layer longitudinal dielectric susceptibilities

By taking into account of the applied longitudinal electric field E, the layer longitudinal polarizations take the form

$$p_{nz} = 2^{-N-2N_0} \sum_{\mu=0}^{N} \sum_{\mu_1=0}^{N_0} \sum_{\mu_2=0}^{N_0} \{C_\mu^N C_{\mu_1}^{N_0} C_{\mu_2}^{N_0} (1-2p_{nz})^{\mu} (1+2p_{nz})^{N-\mu} (1-2p_{n-1,z})^{\mu_1} \times (1+2p_{n-1,z})^{N_0-\mu_1} (1-2p_{n+1,z})^{\mu_2} (1+2p_{n+1,z})^{N_0-\mu_2} f_z(y_n+E,\Omega)\} \quad (A.1)$$

with the periodic boundary conditions

$$p_{nz}(n=0) = p_n z(n=L),$$
$$p_{nz}(n=L+1) = p_{nz}(n=1),$$
$$L = L_A + L_B$$

and where

$$y_n = \tfrac{1}{2}[J_{nn}(N-2\mu) + J_{n,n-1}(N_0 - 2\mu_1) + J_{n,n+1}(N_0 - 2\mu_2)]. \tag{A.2}$$

By differentiating the equation of the layer longitudinal polarization (Eq. (A.1)), with respect to E and taking the limit when E goes to zero, we get the following:

$$\frac{\partial p_{nz}}{\partial E}\Big)_{E=0} = A^z_{n,n-1}\frac{\partial p_{n-1,z}}{\partial E}\Big)_{E=0} + A^z_{n,n}\frac{\partial p_{nz}}{\partial E}\Big)_{E=0} + A^z_{n,n+1}\frac{\partial p_{n+1,z}}{\partial E}\Big)_{E=0} + B^z_n. \tag{A.3}$$

Eq. (A.3) yields

$$C^z_{n,n-1}\chi_{n-1,z} + C^z_{n,n}\chi_{nz} + C^z_{n,n+1}\chi_{n+1,z} = 1 \tag{A.4}$$

with

$$C^z_{n,n-1} = -\frac{A^z_{n,n-1}}{B^z_n}, \quad C^z_{n,n} = \frac{1 - A^z_{n,n}}{B^z_n}, \quad C^z_{n,n+1} = -\frac{A^z_{n,n+1}}{B^z_n}$$

with the periodic boundary conditions $C_{1,0} = C_{1,L}$ and $C_{L,L+1} = C_{L,1}$.

Eq. (A.4) is a set of L linear equations from which the layer longitudinal susceptibilities are obtained. The expressions of the coefficients appearing in the equations of the appendix are given by

$$\begin{aligned} A^z_{n,n-1} = {} & 2^{-N-2N_0}\sum_{\mu=0}^{N}\sum_{\mu_1=0}^{N_0}\sum_{\mu_2=0}^{N_0}\sum_{i=0}^{\mu_1}\sum_{j=0}^{N_0-\mu_1}\{C^N_\mu C^{N_0}_{\mu_1} C^{\mu_1}_i C^{N_0-\mu_1}_j(-1)^i 2^{i+j}(i+j) \\ & \times (p_{n-1,z})^{i+j-1}(1-2p_{nz})^{\mu}(1+2p_{nz})^{N-\mu}(1-2p_{n+1,z})^{\mu_2}(1+2p_{n+1,z})^{N_0-\mu_2} \\ & \times f_z(y_n,\Omega)\}, \end{aligned} \tag{A.5}$$

$$\begin{aligned} A^z_{n,n} = {} & 2^{-N-2N_0}\sum_{\mu=0}^{N}\sum_{\mu_1=0}^{N_0}\sum_{\mu_2=0}^{N_0}\sum_{i=0}^{\mu}\sum_{j=0}^{N-\mu}\{C^N_\mu C^{N_0}_{\mu_1} C^{\mu}_i C^{N-\mu}_j(-1)^i 2^{i+j}(i+j) \\ & \times (p_{nz})^{i+j-1}(1-2p_{n-1,z})^{\mu_1}(1+2p_{n-1,z})^{N_0-\mu_1}(1-2p_{n+1,z})^{\mu_2}(1+2p_{n+1,z})^{N_0-\mu_2} \\ & \times f_\alpha(y_n,\Omega)\}, \end{aligned} \tag{A.6}$$

$$\begin{aligned} A^z_{n,n+1} = {} & 2^{-N-2N_0}\sum_{\mu=0}^{N}\sum_{\mu_1=0}^{N_0}\sum_{\mu_2=0}^{N_0}\sum_{i=0}^{\mu_1}\sum_{j=0}^{N_0-\mu_2}\{C^N_\mu C^{N_0}_{\mu_1} C^{\mu_2}_i C^{N_0-\mu 2}_j(-1)^i 2^{i+j}(i+j) \\ & \times (p_{n+1,z})^{i+j-1}(1-2p_{nz})^{\mu}(1+2p_{nz})^{N-\mu}(1-2p_{n-1,z})^{\mu_1}(1+2p_{n-1,z})^{N_0-\mu 1} \\ & \times f_\alpha(y_n,\Omega)\}, \end{aligned} \tag{A.7}$$

$$\begin{aligned} B^z_n = {} & 2^{-N-2N_0}\sum_{\mu=0}^{N}\sum_{\mu_1=0}^{N_0}\sum_{\mu_2=0}^{N_0} C^N_\mu C^{N_0}_{\mu_1} C^{N_0}_{\mu_2}(1-2p_{nz})^{\mu}(1+2p_{nz})^{N-\mu}(1-2p_{n-1,z})^{\mu_1} \\ & \times (1+2p_{n-1,z})^{N_0-\mu_1}(1-2p_{n+1,z})^{\mu_2}(1+2p_{n+1,z})^{N_0-\mu_2} g_z(y_n,\Omega), \end{aligned} \tag{A.8}$$

where the function $g_z(y,\Omega)$ is given by

$$\begin{aligned} g_z(y,\Omega) = \frac{\partial f_z(y,\Omega)}{\partial E}\Big)_{E=0} = {} & \frac{1}{2}\left\{\frac{\Omega^2}{(y^2+\Omega^2)^{\frac{3}{2}}}\tanh\left[\frac{1}{2}\beta(y^2+\Omega^2)^{\frac{1}{2}}\right]\right. \\ & \left. + \frac{\beta}{2}\frac{y^2}{(y^2+\Omega^2)}\left\{1-\tanh^2\left[\frac{1}{2}\beta(y^2+\Omega^2)^{\frac{1}{2}}\right]\right\}\right\}. \end{aligned} \tag{A.9}$$

A.1. Calculation of the layer pyroelectric coefficient

By differentiating the equations of the layer longitudinal polarizations (Eq. (A.1)) with respect to T, we get the following set of equations:

$$\frac{\partial p_{nz}}{\partial T} = A^z_{n,n-1}\frac{\partial p_{n-1,z}}{\partial T} + A^z_{n,n}\frac{\partial p_{nz}}{\partial T} + A^z_{n,n+1}\frac{\partial p_{n+1,z}}{\partial T} + D^z_n. \tag{A.10}$$

The set of Eqs. (A.10) yields

$$E^z_{n,n-1}\chi_{n-1,z} + E^z_{n,n}\chi_{nz} + E^z_{n,n+1}\chi_{n+1,z} = 1 \quad \text{for } 1 \leqslant n \leqslant L \tag{A.11}$$

with

$$E^z_{n,n-1} = -\frac{A^z_{n,n-1}}{D^z_n}, \quad E^z_{n,n} = \frac{1 - A^z_{n,n}}{D^z_n}, \quad E^z_{n,n+1} = -\frac{A^z_{n,n+1}}{D^z_n}.$$

Eq. (A.11) are a set of L linear equations from which the layer longitudinal dielectric susceptibilities are obtained. The expressions of the coefficients appearing in the equations of the appendix are given by

$$\begin{aligned} D^z_n = {} & 2^{-N-2N_0}\sum_{\mu=0}^{N}\sum_{\mu_1=0}^{N_0}\sum_{\mu_2=0}^{N_0} C^N_\mu C^{N_0}_{\mu_1} C^{N_0}_{\mu_2}(1-2p_{nz})^{\mu}(1+2p_{nz})^{N-\mu}(1-2p_{n-1,z})^{\mu_1} \\ & \times(1+2p_{n-1,z})^{N_0-\mu_1}(1-2p_{n+1,z})^{\mu_2}(1+2p_{n+1,z})^{N_0-\mu_2} h_z(y_n, \Omega_n), \end{aligned} \tag{A.12}$$

where the function $h_z(y, \Omega)$ is given by

$$h_z(y,\Omega) = \frac{\partial f_z(y,\Omega)}{\partial T} = -\beta^2\frac{y}{4}\left\{1 - \tanh^2\left[\frac{1}{2}\beta(y^2+\Omega^2)^{1/2}\right]\right\}. \tag{A.13}$$

References

[1] D.R. Tilley, B. Zeks, Solid State Commun. 49 (1984) 823.
[2] K. Binder, Ferroelectrics. 73 (1987) 43.
[3] C.L. Wang, W.L. Zhong, P.L. Zhang, J. Phys. Condens. Matter 3 (1992) 4743.
[4] C.B. Parker, J.P. Maria, A.I. Kingon, Appl. Phys. Lett. 81 (2002) 340.
[5] C.S. Hwang, J. Appl. Phys. 92 (2002) 432.
[6] J.F. Scott, Ferroelect. Rev. 1 (1998) 1.
[7] X.L. Zhong, Y.G. Wang, P.L. Zhang, Ferroelect. Rev. 131 (1998) 1.
[8] E.K. Tan, J. Osman, D.R. Tilley, Solid State Commun. 116 (2000) 61.
[9] D.R. Tilley, Solid State Commun. 65 (1988) 657.
[10] D. Schwenk, F. Fishman, F. Schawble, Ferroelectrics 104 (1990) 349.
[11] B.D. Qu, W.L. Zhong, R.H. Prince, Phys. Rev. B 55 (1997) 11218.
[12] Y.Q. Ma, J. Shen, X.H. Xu, Solid State Commun. 114 (2000) 461.
[13] M.D. Glinchuk, E.A. Eliseev, V.A. Stephanovich, M.G. Karkut, R. Farhi, Preprint Cond-mat/0004258
[14] C.L. Wang, S.P.R. Smith, J. Kor. Phys. Soc. 32 (1998) S382.
[15] X.G. Wang, S.H. Pan, G.Z. Yang, J. Phys. 11 (1999) 6581.
[16] R. Blink, B. Zeks, Soft Modes in Ferroelectrics and Antiferroelectrics, North-Holland Publ, Co, Amsterdam, 1974.
[17] R.J. Elliott, G.A. Gehring, A.P. Malozemoff, S.P. Smith, N.S. Staude, R.N. Tyte, J. Phys. C 4 (1971) L179.
[18] Y.L. Wang, B. Cooper, Phys. Rev. 172 (1968) 539.
[19] R.B. Stinchcombe, J. Phys. C. 6 (1973) 2459.
[20] J.F. Webb, Science Progress. 86 (2003) 203.
[21] M. E. Lines, A. M. Glass, (Eds.), Principles and Applications of Ferroelectrics and Related Materials, Oxford University Press, Oxford, re-issue 2001.
[22] M. Saber, Chin. J. Phys. 35 (1997) 577.
[23] C. Wang, D.R. Tilley, Solid State Commun. 118 (2001) 333.
[24] F. Dujardin, B. Stébé, A. Ainane, M. Saber, Physica A 269 (1999) 322.
[25] A.R. Ferchmin, W. Maciejewski, J. Phys. C. 12 (1979) 4311.
[26] C.L. Wang, S.R.P. Smith, D.R. Tilley, J. Phys. Condens. Matter 6 (1994) 9633.
[27] Y. Xin, C.L. Wang, W.L. Zhong, P.L. Zhang, Solid State Commun. 110 (1999) 265.

[28] J.P. Remeika, A.M. Glass, Mater. Res. Bull. 5 (1970) 37.
[29] C.L. Wang, Y. Xin, X.S. Wang, W.L. Zhong, P.L. Zhang, Phys. Lett. A 268 (2000) 117.
[30] B.D. Qu, M. Evstigneev, D.J. Johnson, R.H. Prince, Appl. Phys. Lett. 72 (1998) 1394.
[31] C.A. Ramos, D. Lederman, A.R. King, V. Jaccarino, Phys. Rev. Lett. 65 (1990) 2913.
[32] A.S. Carrico, R.E. Camley, Phys. Rev. B 45 (1992) 13117.
[33] R.W. Wang, D.L. Mills, Phys. Rev. B. 46 (1992) 11681.